

Propagation Characteristics of Flexural Wave in One-Dimensional Phononic Crystals Based on Lattice Dynamics Model

Hao Wu¹, Youdi Kuang^{1,2*}

¹School of Mechanics and Construction Engineering, MOE Key Laboratory of Disaster Forecast and Control in Engineering, Jinan University, Guangzhou, China

²School of Civil Engineering and Architecture, Wuyi University, Jiangmen, China

Email: *kuangzhang88@gmail.com

How to cite this paper: Wu, H. and Kuang, Y.D. (2022) Propagation Characteristics of Flexural Wave in One-Dimensional Phononic Crystals Based on Lattice Dynamics Model. *Journal of Applied Mathematics and Physics*, 10, 1416-1431.
<https://doi.org/10.4236/jamp.2022.105100>

Received: March 28, 2022

Accepted: May 6, 2022

Published: May 9, 2022

Copyright © 2022 by author(s) and Scientific Research Publishing Inc. This work is licensed under the Creative Commons Attribution International License (CC BY 4.0).

<http://creativecommons.org/licenses/by/4.0/>



Open Access

Abstract

In this paper, we establish discrete flexural lattice chain models of Bragg and locally resonant phononic crystals by setting mass defect atoms and local resonant elements on the flexural lattice chain. The bandgap characteristics of flexural wave in phononic crystals are studied by establishing the governing equations of the model. The results from models show that with the change of the mass ratio of defective atoms to normal atoms, the bandgap of the flexural wave produced by Bragg scattering shows a certain rule. When the local resonant bandgap and Bragg scattering bandgap are close to each other, the two bandgaps will be coupled to form a wider flexural wave bandgap. The effect of axial strain on bending wave propagation is only the shift of bandgap position. The effect of material damping on the propagation of a bending wave is only energy dissipation at high frequency. In addition, we use finite element simulation to calculate the bandgap of flexural wave in phononic crystals with mass defects, and the results are consistent with lattice chain model. This shows that lattice chain model can effectively guide the bandgap design of phononic crystals. This comprehensive study may help to elucidate the rule of bandgap generation of flexural wave in one-dimensional phononic crystals.

Keywords

Phononic Crystals, Local Resonance, Bragg Scattering, Damping, Strain, Flexural Wave

1. Introduction

Phononic crystals (PCs) [1] are periodic composites with elastic wave bandgaps. Elastic wave in the bandgap frequency range cannot propagate. Due to this cha-

racteristic, PCs have received extensive attention in recent years and have also generated many applications, such as vibration isolation and noise reduction [2] [3], filters and waveguides [4] [5].

PCs generate bandgaps mainly through the Bragg scattering mechanism [6] and local resonance mechanism [7]. For the former, the Bandgaps are generated by the interaction between periodic structures and elastic wave. For the latter, the Bandgaps are generated by elastic wave resonating with a scatterer. At present, simplified models of PCs have been established based on continuum theory. Based on these models, the bandgap characteristics of PCs are studied extensively. Sigalas [8] studied the effect of density difference between matrix and scatterer on elastic wave propagation. Vasseur [9] studied the influence of elastic modulus difference between matrix and scatterer on elastic wave propagation. Based on Euler beam theory, Wang [10] calculated the band structure of the flexural wave of a locally resonant beam with an infinite period. Gei [11] studied the influence of tensile strain on elastic wave transmission characteristics of quasi-periodic structures. Hussien [12] [13] studied the dissipation of elastic wave energy in the elastic structure with periodic damping and established a theoretical system of wave scattering research based on his research model. Different from the methods based on continuity theory, the PCs discrete lattice dynamics model can provide intuitive and concise insights into wave propagation through simple mechanical models. For example, the propagation characteristics of p-wave can be well proved by the lattice dynamics model [14] and particle models [15]. However, such models are lacking for flexural wave. Motivated by this, we build a flexural lattice chain model of PCs, which can provide more intuitive and basic insights for the design of flexural wave bandgaps in PCs, and effectively save computational costs.

The structure of this paper is as follows: Firstly, the establishment of a one-dimensional flexural lattice chain model is introduced. Secondly, a lattice chain model containing mass defect atoms and local resonators is established, and the effect of model parameters on the flexural wave bandgap is investigated. Then, a finite length lattice chain model with mass defect atoms and the locally resonant unit is established, and the effects of axial strain and damping on the vibrational response of lattice chains are studied. Finally, make a concluding comment.

2. Theoretical Basis

Figure 1(a) shows the lattice chain model of a one-dimensional structure. m denotes atomic mass, a denotes the lattice constant, k_a the rotational stiffness of the rod, θ denotes the corner of the rod. **Figure 1(b)** shows the displacement diagram of atoms in the flexural vibration of one-dimensional lattice chains, y denotes the displacement of the atom in the y -direction. **Figure 1(c)** shows the force analysis of the rod, M_i ($i = n - 1, n, n + 1$) denotes the bending moment. Q_L, Q_R denotes the shear force. **Figure 1(d)** shows the force analysis of the atom.

According to geometric conditions, the angle changes of the two rods in **Figure 1(c)** can be expressed as:

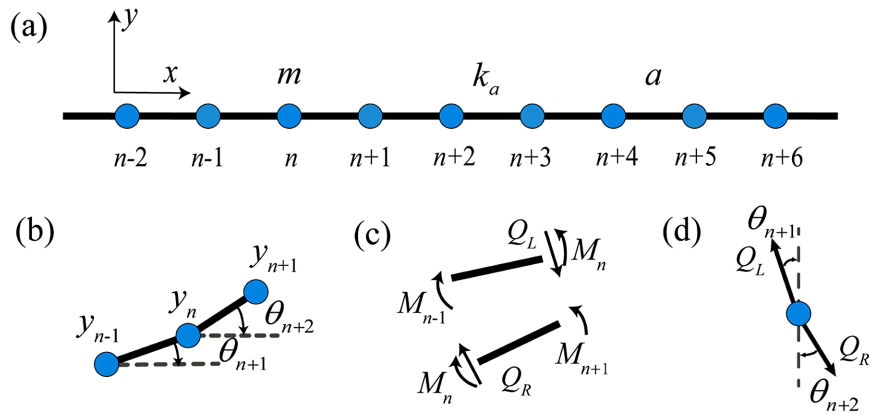


Figure 1. One-dimensional monatomic lattice chain and its force analysis.

$$\sin \theta_{n+1} \approx \theta_{n+1} = \frac{y_n - y_{n-1}}{a} \tag{1}$$

$$\sin \theta_{n+2} \approx \theta_{n+2} = \frac{y_{n+1} - y_n}{a}$$

The bending moment in figure (d) is expressed as:

$$\begin{aligned} M_{n-1} &= k_a (\theta_n - \theta_{n-1}) = k_a \frac{y_{n-2} + y_n - 2y_{n-1}}{a} \\ M_n &= k_a (\theta_{n+1} - \theta_n) = k_a \frac{y_{n-1} + y_{n+1} - 2y_n}{a} \\ M_{n+1} &= k_a (\theta_{n+2} - \theta_{n+1}) = k_a \frac{y_n + y_{n+2} - 2y_{n+1}}{a} \end{aligned} \tag{2}$$

The moment balance equation can be expressed as:

$$\begin{aligned} Q_L \cdot a + M_{n-1} &= M_n \\ Q_R \cdot a + M_n &= M_{n+1} \end{aligned} \tag{3}$$

According to Newton's second law, the governing equation of n -atom bending vibration is written as:

$$m \frac{d^2 y_n}{dt^2} = Q_L - Q_R = \frac{2M_n - M_{n+1} - M_{n-1}}{a} \tag{4}$$

Substituting (1), (2) and (3) into (4), we can get the governing equation for n atom:

$$m \frac{d^2 y_n}{dt^2} = k_a (4y_{n+1} + 4y_{n-1} - 6y_n - y_{n-2} - y_{n+2}) \tag{5}$$

3. Band Structure of One-Dimensional Phononic Crystals Lattice Chain Model

3.1. Calculation of Band Structure of Lattice Chains with Mass Defects

Figure 2 shows the lattice chain model of mass defect PCs and their unit cell structure. The red atom is a mass defect atom with a mass of m_1 . The blue atom has mass m_2 .

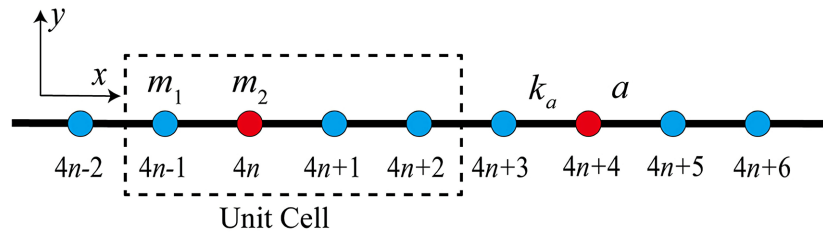


Figure 2. Lattice chain unit cell structure.

According to the introduction of the theoretical basis, the governing equation of atoms in unit cell can be written as:

$$\begin{aligned}
 m_1 \frac{d^2 y_{4n-1}}{dt^2} &= \frac{k_a}{a^2} (4y_{4n-2} + 4y_{4n} - 6y_{4n-1} - y_{4n+1} - y_{4n-3}) \\
 m_2 \frac{d^2 y_{4n}}{dt^2} &= \frac{k_a}{a^2} (4y_{4n-1} + 4y_{4n+1} - 6y_{4n} - y_{4n+2} - y_{4n-2}) \\
 m_1 \frac{d^2 y_{4n+1}}{dt^2} &= \frac{k_a}{a^2} (4y_{4n} + 4y_{4n+2} - 6y_{4n+1} - y_{4n+3} - y_{4n-1}) \\
 m_1 \frac{d^2 y_{4n+2}}{dt^2} &= \frac{k_a}{a^2} (4y_{4n+1} + 4y_{4n+3} - 6y_{4n+2} - y_{4n+4} - y_{4n})
 \end{aligned} \tag{6}$$

According to Bloch’s theorem, the lattice wave solution in a lattice chain can be written as:

$$\begin{aligned}
 y_{4n-1} &= Ae^{i(\omega t + 4nka)} \\
 y_{4n} &= Be^{i[\omega t + (4n+1)ka]} \\
 y_{4n+1} &= Ce^{i[\omega t + (4n+2)ka]} \\
 y_{4n+2} &= De^{i[\omega t + (4n+3)ka]}
 \end{aligned} \tag{7}$$

where A, B, C and D represent the maximum displacement of atoms $4n - 1, 4n, 4n + 1$ and $4n + 2$ in the y -direction respectively. t denotes the time, ω denotes the frequency, k denotes wave vector. Substituting (7) into (6) and solving the eigenvalue problem, the relation between wave vector k and frequency can be obtained. By plugging in the data $k_a = 1, a = 1, m_1 = 1, m_2 = 2$ (dimensionless), the bandgap of a one-dimensional lattice chain can be obtained, as shown in **Figure 3**.

Figure 3 shows the relationship between frequency and wave vector in a lattice chain with a mass defect atom. The band structure consists of four curves. The bottom curve is an acoustic branch. The rest is an optical branch. The shaded part is the bandgap of the flexural wave caused by Bragg scattering.

The main cause for the bandgap is the material density difference between matrix and scatter in PCs. To clarify the effect of this difference on the bandgap of the flexural wave through the existing lattice chain model, we calculate the band structure of the lattice chain under different parameters by changing the value of atomic mass ratio m_2/m_1 . **Figure 4** shows the starting frequency, cutoff frequency and bandgap width of the first bandgap, second bandgap and third bandgap of the band structure under different m_2/m_1 .

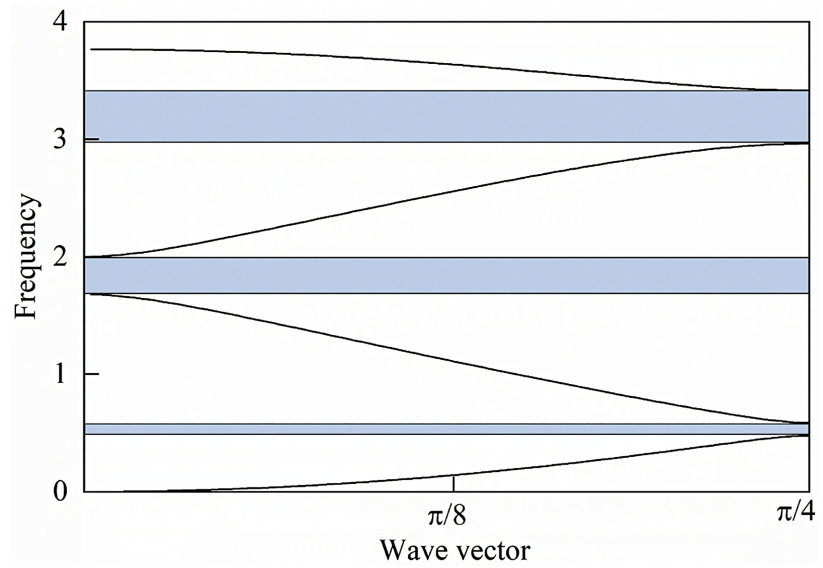
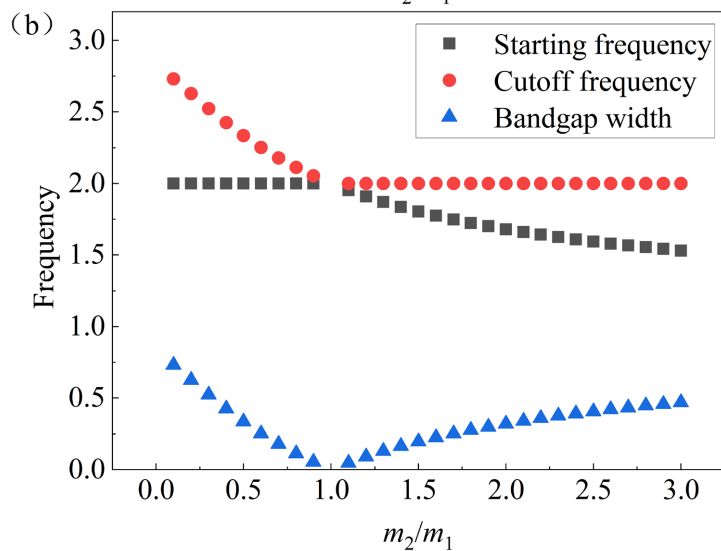
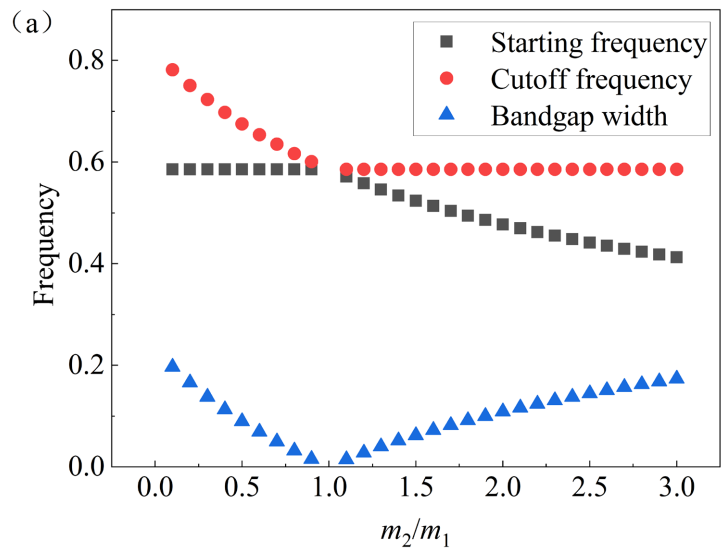


Figure 3. Mass defect lattice chain band structure.



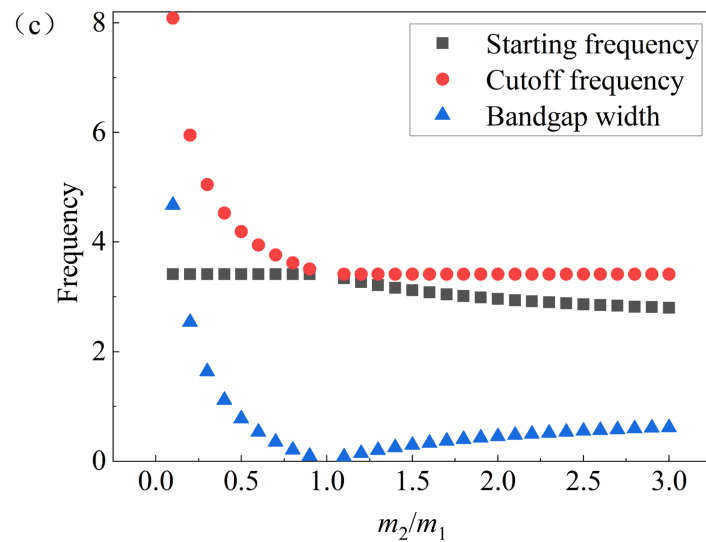


Figure 4. Band structure of mass defect lattice chain at different m_2/m_1 .

Figures 4(a)-(c) respectively show the starting frequencies, cutoff frequencies and bandgap widths of the first bandgap, second bandgap and third bandgap of the lattice chain band structure at different m_2/m_1 . When $m_2/m_1 < 1$, with the increase of m_2/m_1 , the starting frequency remains unchanged, the cutoff frequency decreases and the frequency range decreases. When $m_2/m_1 > 1$, with the increase of m_2/m_1 , the starting frequency decreases, the cutoff frequency stays constant and the frequency range increases. From the point of view of bandgap width, when the atomic mass difference is larger, the bandgap is wider. From the point of view of the bandgap position, the initial frequency of the bandgap at $m_2/m_1 < 1$ is consistent with the cutoff frequency of the bandgap at $m_2/m_1 > 1$ and the magnitude of this frequency is determined by the lattice constant. This means that when $m_2/m_1 < 1$, the elastic wave bandgap with a higher frequency will be obtained, and when $m_2/m_1 > 1$, the elastic wave bandgap with a lower frequency will be obtained. This is of great significance to the design of the flexural bandgap in PCs.

In addition, we use finite element simulation to calculate the band structure of PCs with quality defects to verify the lattice chain model. Firstly, we established the PCs unit cell finite element model as shown in **Figure 5**. Where, $a = 10$ mm, $b = 2$ mm, red and yellow represent materials A and B respectively. The two materials have the same Young's modulus ($E = 71$ GPa) and Poisson's ratio ($\mu = 0.33$), but different densities ($\rho_A = 2700$ kg/m³). By adjusting the density of material B, we can get the relationship between ρ_B/ρ_A and the starting frequency, cutoff frequency and bandgap width of the first bandgap, second bandgap and third bandgap in the band structure, as shown in **Figure 6**.

By comparing **Figure 5** and **Figure 6**, we found that with the change of quality defects, the band gap changes in the lattice chain model and the finite element simulation results are consistent. This indicates that lattice chain model can effectively guide the design of PCs flexural bandgap.

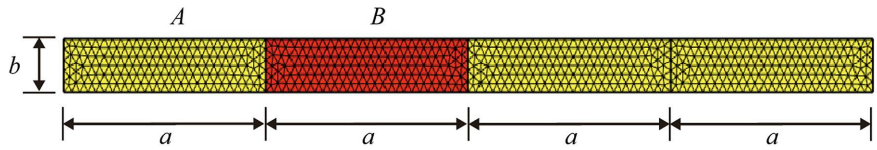


Figure 5. PCs unit cell finite element model.

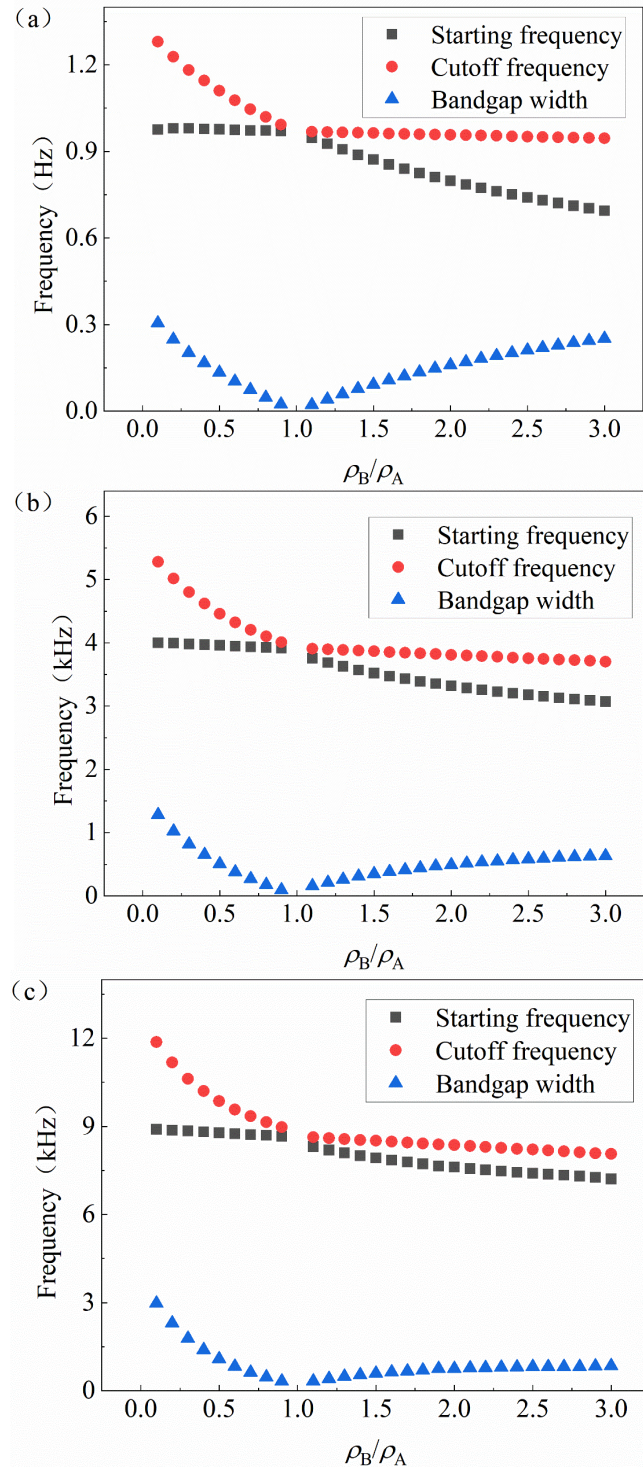


Figure 6. Banded structures of PCs with mass defects at different ρ_B/ρ_A .

3.2. Calculation of Band Structure of Lattice Chains with Locally Resonant Unit

Figure 7 shows the lattice chain model of locally resonant PCs and their unit cell structure. k_b denotes the spring stiffness of the local resonance unit, m' denotes atomic mass of locally resonant unit.

According to Newton's second law, the equilibrium equation for atom 1' is:

$$m' \frac{d^2 y_{1'}}{dt^2} = -k_b (y_{1'} - y_0) \tag{8}$$

The vibrational solution of 1' atom is as follows:

$$y_{1'} = A_1 \cos(\omega t + \varphi) \tag{9}$$

A_1 denotes the maximum amplitude of 1' atom, ω denotes the frequency of vibration, φ denotes the phase. According to the introduction of the theoretical basis, the governing equation for $4n$ atom can be obtained:

$$m \frac{d^2 y_{4n}}{dt^2} = \frac{k_a}{a^2} (4y_{4n-1} + 4y_{4n+1} - 6y_{4n} - y_{4n+2} - y_{4n-2}) + k_b (y_{1'} - y_{4n}) \tag{10}$$

Substituting (8) and (9) into (10), and the governing equation for $4n$ -atom becomes:

$$m \frac{d^2 y_{4n}}{dt^2} = \frac{k_a}{a^2} (4y_{4n-1} + 4y_{4n+1} - 6y_{4n} - y_{4n+2} - y_{4n-2}) + \frac{m\omega^2 k_b}{k_b - m\omega^2} y_{4n} \tag{11}$$

The governing equation of atoms in unit cell can be written as:

$$\begin{aligned} m \frac{d^2 y_{4n-1}}{dt^2} &= \frac{k_a}{a^2} (4y_{4n-2} + 4y_{4n} - 6y_{4n-1} - y_{4n+1} - y_{4n-3}) \\ m \frac{d^2 y_{4n}}{dt^2} &= \frac{k_a}{a^2} (4y_{4n-1} + 4y_{4n+1} - 6y_{4n} - y_{4n+2} - y_{4n-2}) + \frac{m\omega^2 k_b}{k_b - m\omega^2} y_{4n} \\ m \frac{d^2 y_{4n+1}}{dt^2} &= \frac{k_a}{a^2} (4y_{4n} + 4y_{4n+2} - 6y_{4n+1} - y_{4n+3} - y_{4n-1}) \\ m \frac{d^2 y_{4n+2}}{dt^2} &= \frac{k_a}{a^2} (4y_{4n+1} + 4y_{4n+3} - 6y_{4n+2} - y_{4n+4} - y_{4n}) \end{aligned} \tag{12}$$

The Lattice solution can also be expressed as Equation (7).

Substituting (7) into (12) and solving the eigenvalue problem, the relation between wave vector k and frequency can be obtained. By plugging in the data $k_a = 1, k_b = 1, a = 1, m = 1, m' = 1$ the bandgap of a one-dimensional lattice chain can be obtained, as shown in Figure 6.

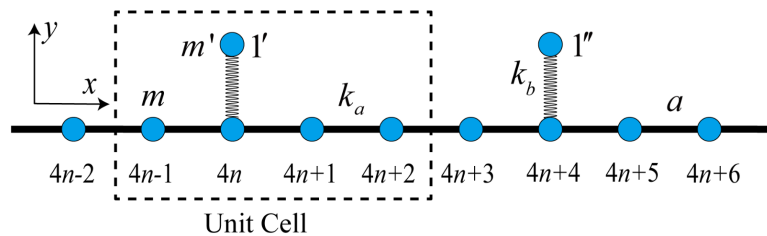


Figure 7. Lattice chain unit cell structure.

Figure 8 shows the relationship between frequency and wave vectors in a lattice chain with locally resonant units. The shaded part is the bandgap of the flexural wave caused by the local resonance of Bragg scattering. Since the local resonance unit increases the equivalent mass of the atom to which it is attached. The periodic existence of mass defect atoms in the lattice chain leads to the appearance of Bragg scattering bandgaps in the band structure. The local resonant bandgap is generated because the flexural wave resonates in the local resonant element, and its bandgap position is related to the resonant frequency.

The position and width of the bandgap in locally resonant PCs are closely related to the resonant frequency of the locally resonant unit. We calculate the band structure of lattice chains with different local resonant frequencies ω by changing the value of k_b in the local resonant unit. **Figure 9** shows the band structure of flexural wave at different ω .

Figure 9 shows the band structure of lattice chains at different resonant frequencies ω . The shaded areas represent the flexural wave bandgap. We can see that with the change of the local resonant frequency, the position of the local resonant bandgap of the flexural wave also changes. As the local resonant frequency increases, the Bragg scattering bandgap also increases. This is due to the increase in the equivalent mass of the $4n$ atom as the resonance frequency increases (k_a or m' increases). By comparing **Figure 9(g)**, **Figure 9(h)** and **Figure 3**. We find that when the local resonant frequency is large, the local resonant bandgap disappears and the band structures of the mass defect type and the local resonance type lattice chains are consistent under specific parameters. This shows that when the stiffness of the local resonant unit spring is too large, local resonant PCs will be transformed into Bragg scattering PCs. By comparing the band structure in **Figure 9**, we also find that when the Bragg bandgap and the local resonant bandgap are close to each other, a wider flexural wave bandgap is formed through coupling.

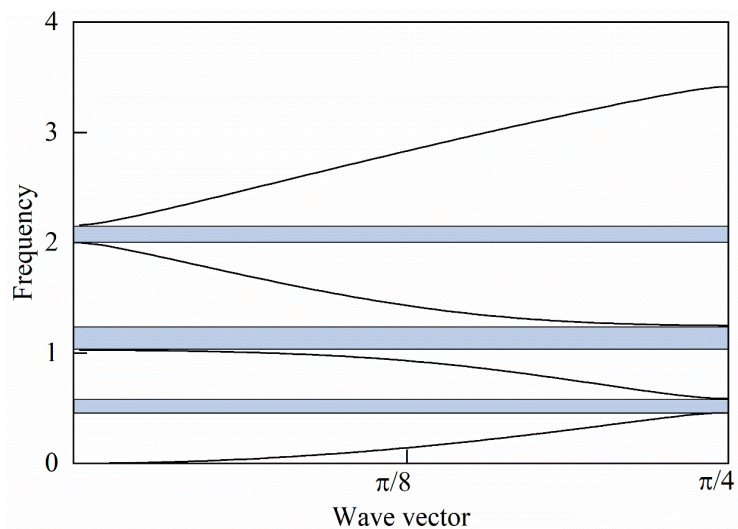


Figure 8. Lattice chain band structure.

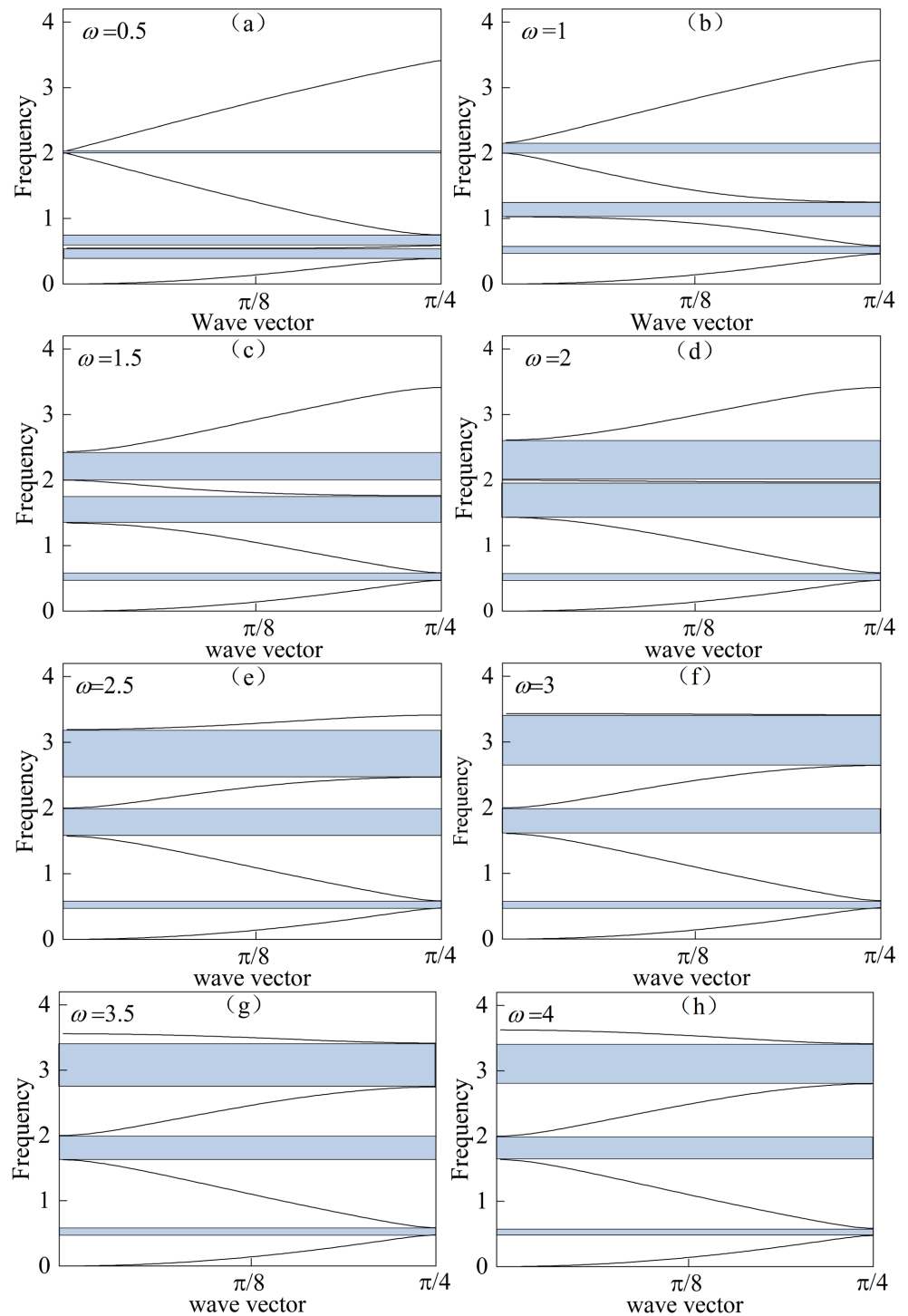


Figure 9. Lattice chain band structure at different ω .

4. Amplitude-Frequency Response of Lattice Chain Model of One-Dimensional Phononic Crystals

The band structure is calculated based on infinite period, but there is no infinite period structure in reality. So, it is very important to calculate the amplitude-frequency response of the finite period structure. In this chapter, we calculate

the amplitude-frequency response of the flexural vibration of a one-dimensional finite lattice chain model and investigate the effects of axial tension and material damping on the bandgap of flexural vibration.

4.1. Amplitude-Frequency Response Calculation

In this section, we introduce the amplitude-frequency response calculation of the PCs lattice chain model with 10-unit cells.

Figure 10 shows a lattice chain model with 10 mass-defect atoms (red atoms). The mass defect atoms are spaced $4a$. A harmonic displacement excitation in the y -direction is applied to the left end of the lattice chain, and the other end is kept free. We can establish the governing equation of atom by Newton's second law and bending moment balance:

$$\begin{aligned}
 y_1 &= A \sin(\omega t) \\
 m_1 \frac{d^2 y_2}{dt^2} &= \frac{k_a}{b^2} (3y_1 - 6y_2 + 4y_3 - y_4) \\
 m_1 \frac{d^2 y_{42}}{dt^2} &= \frac{k_a}{b^2} (3y_{43} - 6y_{42} + 4y_{41} - y_{40}) \\
 m_1 \frac{d^2 y_{43}}{dt^2} &= \frac{k_a}{b^2} (-2y_{43} + 3y_{42} - y_{41})
 \end{aligned} \tag{13}$$

when $3 \leq n \leq 41$ the governing equation for the blue atom can be expressed as:

$$m_1 \frac{d^2 y_n}{dt^2} = \frac{k_a}{a^2} (4y_{n-1} + 4y_{n+1} - 6y_n - y_{n-2} - y_{n+2}) \tag{14}$$

when $3 \leq n \leq 41$ the governing equation for the red atom can be expressed as:

$$m_2 \frac{d^2 y_n}{dt^2} = \frac{k_a}{a^2} (4y_{n-1} + 4y_{n+1} - 6y_n - y_{n-2} - y_{n+2}) \tag{15}$$

A denotes the amplitude of harmonic excitation; other parameters are consistent with chapter 2.

y_{43} is obtained by solving the governing equations of all atoms in the lattice chain simultaneously. We define the amplitude-frequency response as:

$$T = 20 \times \log_{10} \left(\frac{P_{out}}{P_{in}} \right) \tag{16}$$

P_{out} and P_{in} represent the maximum displacement response of y_1 and y_{43} , respectively. By plugging in the data $k_a = 1$, $a = 1$, $m_1 = 1$, $m_2 = 2$ the amplitude-frequency response of the one-dimensional lattice chain can be obtained, as shown in **Figure 11**.

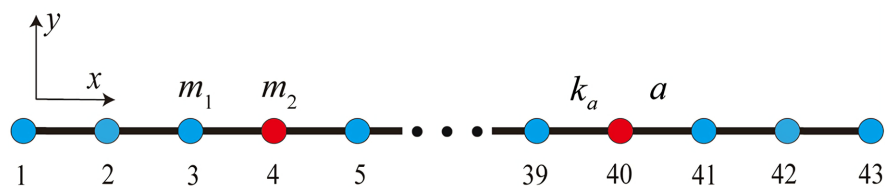


Figure 10. Lattice chain model.

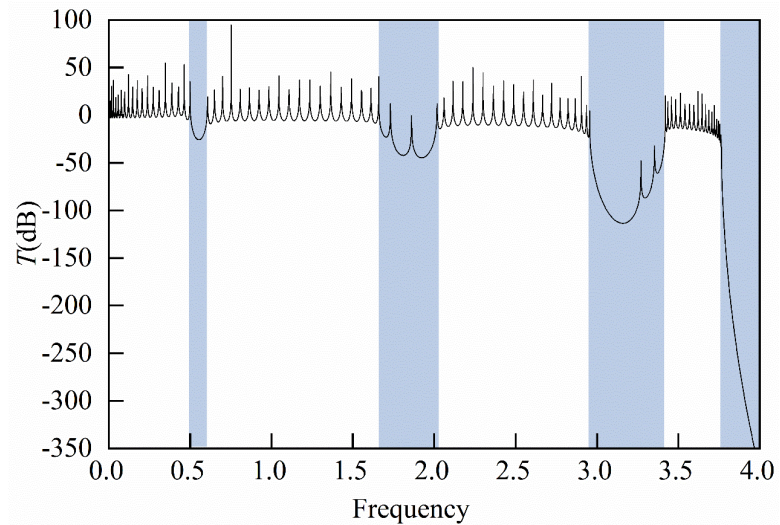


Figure 11. Amplitude-frequency response.

Figure 11 shows the amplitude-frequency response of the lattice chain model. The shaded part represents the attenuation frequency range of bending vibration.

4.2. Effect of Strain on Lattice Chain Bending Vibration

Axial stress is the most common form of stress in one-dimensional structures. It is of great significance to study the effect of axial strain on the bandgap of one-dimensional PCs. In this section, we add axial tensile forces to the finite lattice chain model to calculate the amplitude-frequency response of the lattice chain.

Figure 12 shows the lattice chain model under tension. F donates the axial tensile forces; k_c donates the lattice chain tensile stiffness. We can establish the governing equation of atom by Newton’s second law and bending moment balance:

$$\begin{aligned}
 y_1 &= A \sin(\omega t) \\
 m_1 \frac{d^2 y_2}{dt^2} &= \frac{k_a}{b^2} (3y_1 - 6y_2 + 4y_3 - y_4) + \frac{F}{b} (y_1 - 2y_2 + y_3) \\
 m_1 \frac{d^2 y_{42}}{dt^2} &= \frac{k_a}{b^2} (3y_{43} - 6y_{42} + 4y_{41} - y_{40}) + \frac{F}{b} (y_{41} - 2y_{42} + y_{43}) \\
 m_1 \frac{d^2 y_{43}}{dt^2} &= \frac{k_a}{b^2} (-2y_{43} + 3y_{42} - y_{41}) + \frac{F}{b} (y_{43} - y_{43})
 \end{aligned} \tag{17}$$

when $3 \leq n \leq 41$ the governing equation for the blue atom can be expressed as:

$$m_1 \frac{d^2 y_n}{dt^2} = \frac{k_a}{b^2} (4y_{n-1} + 4y_{n+1} - 6y_n - y_{n-2} - y_{n+2}) + \frac{F}{b} (y_{n+1} - 2y_n + y_{n-1}) \tag{18}$$

when $3 \leq n \leq 41$ the governing equation for the red atom can be expressed as:

$$m_2 \frac{d^2 y_n}{dt^2} = \frac{k_a}{b^2} (4y_{n-1} + 4y_{n+1} - 6y_n - y_{n-2} - y_{n+2}) + \frac{F}{b} (y_{n+1} - 2y_n + y_{n-1}) \tag{19}$$

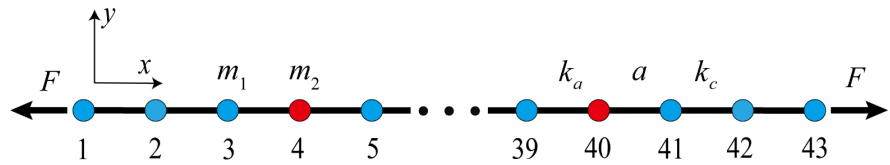


Figure 12. Lattice chain model under tension.

where F denote the axial force, $b = F/k_c$ denote the atomic spacing. The amplitude-frequency response can be obtained by solving the governing equations and equation (16) for all atoms in the lattice chain. By plugging in the data $k_a = 1$, $a = 1$, $m_1 = 1$, $m_2 = 2$ the amplitude-frequency response of the one-dimensional lattice chain can be obtained. By adjusting the axial tension F , we calculated the amplitude-frequency response when strain $\varepsilon = 0.003$ and strain $\varepsilon = 0.006$ respectively, as shown in **Figure 13**.

Figure 13 shows the amplitude-frequency response of finite periodic lattice chains under different strains.

The strain causes the translation of the vibration bandgap generated by Bragg scattering.

4.3. Effect of Damping on Lattice Chain Bending Vibration

Damping is an inherent property of materials, which is related to energy dissipation during vibration, so it is very important to study the effect of damping on PCs vibration characteristics. In this section, damping is added to the lattice chain and the effect of damping on the bandgap of lattice chain bending vibration is studied.

Figure 14 shows the damped lattice chain model, c donates the material damping. We can establish the governing equation of atom by Newton’s second law and bending moment balance:

$$\begin{aligned}
 y_1 &= A \sin(\omega t) \\
 m_1 \frac{d^2 y_2}{dt^2} &= \frac{k_a}{a^2} (3y_1 - 6y_2 + 4y_3 - y_4) + c(y_1 - 2y_2 + y_3) \\
 m_1 \frac{d^2 y_{42}}{dt^2} &= \frac{k_a}{a^2} (3y_{43} - 6y_{42} + 4y_{41} - y_{40}) + c(y_{41} - 2y_{42} + y_{43}) \\
 m_1 \frac{d^2 y_{43}}{dt^2} &= \frac{k_a}{a^2} (-2y_{43} + 3y_{42} - y_{41}) + c(y_{43} - y_{43})
 \end{aligned} \tag{20}$$

when $3 \leq n \leq 41$ the governing equation for the blue atom can be expressed as:

$$m_1 \frac{d^2 y_n}{dt^2} = \frac{k_a}{a^2} (4y_{n-1} + 4y_{n+1} - 6y_n - y_{n-2} - y_{n+2}) + c(y_{n+1} - 2y_n + y_{n-1}) \tag{21}$$

when $3 \leq n \leq 41$ the governing equation for the red atom can be expressed as:

$$m_2 \frac{d^2 y_n}{dt^2} = \frac{k_a}{a^2} (4y_{n-1} + 4y_{n+1} - 6y_n - y_{n-2} - y_{n+2}) + c(y_{n+1} - 2y_n + y_{n-1}) \tag{22}$$

The amplitude-frequency response can be obtained by solving the governing equations and Equation (16) for all atoms in the lattice chain. By plugging in the

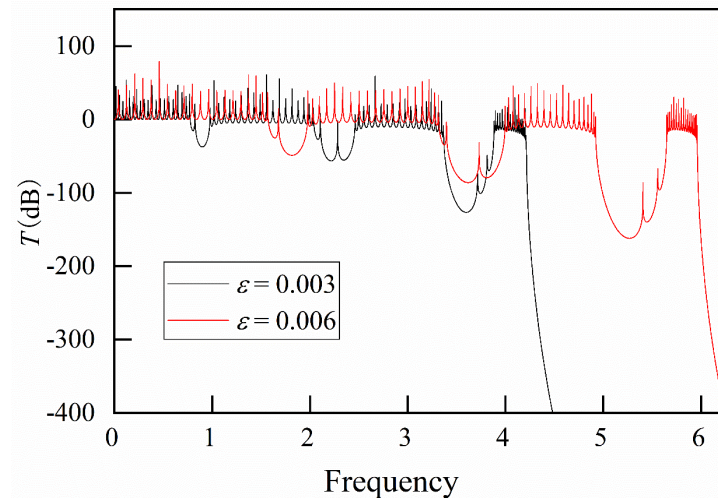


Figure 13. Amplitude-frequency response of lattice chains under tension.



Figure 14. Lattice chain model with damping.

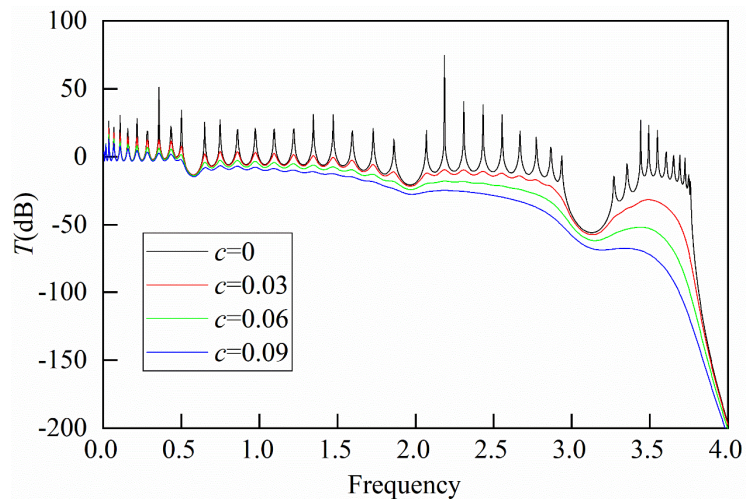


Figure 15. Amplitude-frequency response of lattice chain model with damping.

data $k_a = 1$, $a = 1$, $m_1 = 1$, $m_2 = 2$ the amplitude-frequency response of the one-dimensional lattice chain can be obtained. By adjusting damping c , we calculated the amplitude-frequency response of damping $c = 0.03$, $c = 0.06$ and $c = 0.09$ respectively, as shown in Figure 15.

Figure 15 shows the amplitude-frequency response of finite periodic lattice chains with different damping. When the damping is constant, the attenuation of vibration response caused by damping increases with the increase of displacement excitation frequency. When the displacement excitation frequency is constant, the response attenuation caused by damping increases with the in-

crease of damping.

5. Conclusion

In this paper, the crystal lattice dynamics model of one-dimensional PCs is established and the principles of the Bragg scattering bandgap and local resonant bandgap are revealed from the lattice dynamics perspective. The influence mechanism of mass ratio of mass defect atom to ordinary atom and local resonance frequency on bandgap was investigated. Based on the practical application, the lattice chain model of finite periodic PCs is established. The effects of strain and damping on bending vibration attenuation of finite period PCs are summarized. The comprehensive study may provide fundamental insight on how to modulate bandgaps in one-dimensional continuum PCs. At the same time, the flexural lattice chain model of two-dimensional PCs has important guiding significance for the design of flexural wave bandgaps. These studies will be published in our follow-up research.

Conflicts of Interest

The authors declare no conflicts of interest regarding the publication of this paper.

References

- [1] Kushwaha, M.S., Halevi, P., Dobrzynski, L. and Djafari-Rouhani, B. (1993) Acoustic Band Structure of Periodic Elastic Composites. *Physical Review Letters*, **71**, 2022-2025. <https://doi.org/10.1103/PhysRevLett.71.2022>
- [2] Ma, F.Y., Chen, J.Y. and Wu, J.H. (2019) Three-Dimensional Acoustic Sub-Diffraction Focusing by Coiled Metamaterials with Strong Absorption. *Journal of Materials Chemistry C*, **7**, 5131-5138. <https://doi.org/10.1039/C9TC01243E>
- [3] Chen, Y.J., Wu, B., Li, J., Rudykh, S. and Chen, W.Q. (2020) Low-Frequency Tunable Topological Interface States in Soft Phononic Crystal Cylinders. *International Journal of Mechanical Sciences*, **191**, Article ID: 106098. <https://doi.org/10.1016/j.ijmecsci.2020.106098>
- [4] Sugahara, A., Lee, H., Sakamoto, S. and Takeoka, S. (2019) Measurements of Acoustic Impedance of Porous Materials Using a Parametric Loudspeaker with Phononic Crystals and Phase-Cancellation Method. *Applied Acoustics*, **152**, 54-62. <https://doi.org/10.1016/j.apacoust.2019.03.019>
- [5] Taleb, F. and Darbari, S. (2019) Tunable Locally Resonant Surface-Acoustic-Waveguiding Behavior by Acoustoelectric Interaction in ZnO-Based Phononic Crystal. *Physical Review Applied*, **11**, Article ID: 024030. <https://doi.org/10.1103/PhysRevApplied.11.024030>
- [6] Kushwaha, M.S., Halevi, P., Martínez, G., Dobrzynski, L. and Djafari-Rouhani, B. (1994) Theory of Acoustic Band Structure of Periodic Elastic Composites. *Physical Review B*, **49**, 2313-2322. <https://doi.org/10.1103/PhysRevB.49.2313>
- [7] Liu, Z.Y., Zhang, X.X., Mao, Y.W., *et al.* (2000) Locally Resonant Sonic Materials. *Science*, **289**, 1734-1736. <https://doi.org/10.1126/science.289.5485.1734>
- [8] Sigalas, M.M. (1997) Elastic Wave Band Gaps and Defect States in Two-Dimensional Composites. *The Journal of the Acoustical Society of America*, **101**, 1256-1261.

- <https://doi.org/10.1121/1.418156>
- [9] Vasseur, J.O., Deymier, P.A., Beaugeois, P.Y., Djafari-Rouhani, B. and Prevost, D. (2005) Experimental Observation of Resonant Filtering in a Two-Dimensional Phononic Crystal Waveguide. *Zeitschrift für Kristallographie*, **220**, 829-835. <https://doi.org/10.1524/zkri.2005.220.9-10.829>
- [10] Wang, G., Wen, X.S., Wen, J.H. and Liu, Y.Z. (2006) Quasi-One-Dimensional Periodic Structure with Locally Resonant Band Gap. *Journal of Applied Mechanics*, **73**, 167-170. <https://doi.org/10.1115/1.2061947>
- [11] Gei, M. (2010) Wave Propagation in Quasiperiodic Structures: Stop/Pass Band Distribution and Prestress Effects. *International Journal of Solids and Structures*, **47**, 3067-3075. <https://doi.org/10.1016/j.ijsolstr.2010.07.008>
- [12] Phani, A.S. and Hussein, M.I. (Eds.) (2017) Dynamics of Lattice Materials. John Wiley & Sons, Hoboken. <https://doi.org/10.1002/9781118729588>
- [13] Hussein, M.I. and Frazier, M.J. (2010) Band Structure of Phononic Crystals with General Damping. *Journal of Applied Physics*, **108**, Article ID: 093506. <https://doi.org/10.1063/1.3498806>
- [14] Deymier, P. and Runge, K. (2017) Sound Topology, Duality, Coherence and Wave-Mixing. Springer, Cham.
- [15] Liu, Z.G. and Zhang, J.L. (2019) The Exact Solitary Wave Solutions in Continuity Equation of the One-Dimensional Granular Crystals of Elastic Spheres. *Journal of Applied Mathematics and Physics*, **7**, 2760-2766. <https://doi.org/10.4236/jamp.2019.711189>